

## NET3D Calculation on the Depth of Penetration by a Long-Rod Penetrator with Varying Obliquity

Jong-Bong Kim<sup>1, a</sup> and Hyunho Shin<sup>2, b</sup>

<sup>1</sup>Department of Mechanical and Automotive Engineering, Seoul National University of Science and Technology, 232 Gongneung-ro, Nowon-Gu, Seoul 139-743, Republic of Korea

<sup>2</sup>Department of Materials Engineering, Gangneung-Wonju National University, 7 Jughun-gil, Gangneung, Gangwon-do 210-702, Republic of Korea

<sup>a</sup>jbkim@seoultech.co.kr, <sup>b</sup>hshin@gwnu.ac.kr

**Keywords:** Long-Rod Penetrator; Obliquity; Depth of Penetration; NET3D.

**Abstract.** The effect of the obliquity of a long-rod penetrator on the depth of penetration (DOP) into a witness block has been investigated by NET3D code based on a 3D finite element model with SK constitutive model and polynomial equation of state. The calculation results herein are in general agreement with limited number of experimental data and are very close to the calculation results of the CTH code, both of which are available in the literature. By combining with the present results with existing data, the DOP turns out to decrease rapidly with obliquity up to 30°, decrease relatively slowly up to 70°, and show a saturation behavior thereafter up to 90°.

### Introduction

The high-strain-rate impact and penetration phenomena of materials and structures are important in the areas of armor design, micrometeorite impact on space structures, explosive welding, forming, and hardening of metals. Experimental research on the high-strain-rate impact and penetration behavior of materials is costly and time consuming. Although it offers the most accurate results, the time and cost constraints hardly permit the acquisition of a database with enough variation of parameters to construct unambiguous analytical models. A computational approach overcomes the constraints through step-by-step analysis of any event confined to very short period of time and thus can provide an insight which would be difficult to understand solely from the experimental data. In this sense, many computer codes have been developed including NET3D [1-2] and CTH [3-4] for the numerical analysis of the high-strain-rate phenomena. The accumulation of the experience on a code in versatile areas of high-strain-rate impact and penetration events will be desirable for the reliable application of the code.

In the area of armor design, sensor-activated [5-6] and reactive [7-9] armors have received much interest as means to protect kinetic-energy penetrators and shaped charge jets, respectively. These armors fly metallic plates [2, 10-13] or bars [14-15] toward the incoming penetrator. While the mechanisms such as erosion and breakage of the penetrator are associated, the lateral displacement and rotation of the incoming penetrator are the major mechanisms of the protection of the penetrator, and are qualitatively well correlated to the resultant depth of penetration (DOP) in the witness block [2, 10-16]. Thus, the investigation on the effect of the obliquity of the penetrator on the DOP in the witness block receives a high interest [4, 17-18]. Here we check the reliability of the NET3D code [1-2] in the calculation of the DOP by an oblique long-rod penetrator, and draw out the trend of DOP with obliquity via a systematic parameter study.

### Numerical Analysis

By considering the symmetry of the penetration event on the witness block, only half of the three dimensional space has been discretized as seen in Fig. 1. The length and diameter of the penetrator is 80 and 8 mm, respectively ( $L/D$  ratio of 10), and the dimension of the witness block is shown in Fig. 1

(in mm unit). The velocity of the penetrator toward the witness block was 1.4 km/sec. Except for the front surface of the witness block where the penetrator impacts, the normal displacement of the nodes at all surfaces of the block was confined. The normal displacement of the nodes at longitudinal cross section of the penetrator was also confined.

Tetrahedral elements with the characteristics shown in Table 1 have been used. The element erosion criteria are 2.7 and 1.5 of plastic strain for the penetrator (Tungsten heavy alloy; WHA) and the witness block (Rolled homogeneous armor; RHA), respectively, which were determined by the method shown in Reference 19. No fracture model was employed for the penetrator and witness block.

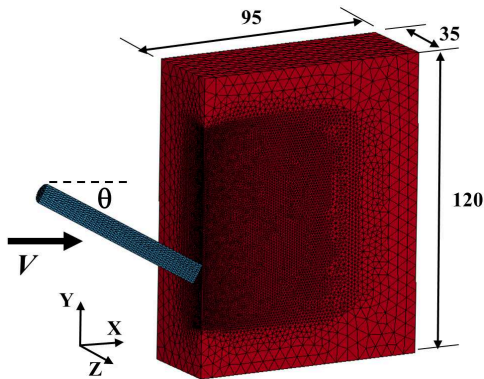


Figure 1 Geometry and mesh of the model.

Table 1. Characteristics of the mesh.

	Penetrator	Target
Total no. of elements	4,514	200,756
No. of elements along diameter	10	NA
No. of elements in peripheral length	14	NA
Min. length (mm)	0.75	0.51

In order to reflect the influence of not only the strain hardening but also the strain-rate hardening and thermal softening, a phenomenological constitutive model [20],

$$\sigma = [A + B\{1 - \exp(-C\varepsilon)\}] [D \ln(\dot{\varepsilon} / \dot{\varepsilon}_0) + \exp(E \cdot \dot{\varepsilon} / \dot{\varepsilon}_0)] \left[ 1 - \frac{T - T_{ref}}{T_m - T_{ref}} \right]^m \quad (1)$$

has been employed, where  $\sigma$ ,  $\varepsilon$ ,  $\dot{\varepsilon}$ ,  $\dot{\varepsilon}_0$ ,  $T_{ref}$  and  $T_m$  are flow stress, strain, strain rate, reference strain rate, reference temperature, and melting temperature, respectively, and  $A$ ,  $B$ ,  $C$ ,  $D$ ,  $E$  and  $m$  are material parameters. Its description capability of the flow stress of many metallic materials is much improved [20-21] than that of the JC model [22]. The model parameters for the WHA penetrator have been determined herein from the experimental data of Reference 23, and those for the RHA witness block from the experimental data of References 24-25, under the assumption of adiabatic deformation of the specimen at the strain rate of  $\geq 1 \text{ sec}^{-1}$  and isothermal deformation below this strain rate. The determined model parameters are shown in Table 2. The reference temperature and reference strain rate were set to be 20°C and 1  $\text{sec}^{-1}$ , respectively.

Table 2 Parameters of the constitutive model (SK).

Parameters	A (MPa)	B (MPa)	C	D	E	m	$T_m$ (°C)
WHA	105.5516	47.1176	9.37	1.3185	0.0	0.2926	1,450
RHA	1,072.0609	717.6717	7.3584	0.0158	0.0	0.9192	1,520

The reduced form of the polynomial model of the equation of state [15] was used for the calculation of the pressure-volume relation:  $P=C_1u$  where  $P$  is the pressure,  $C_1$  is the bulk modulus,  $u=\rho/\rho_0-1$ , and  $\rho/\rho_0$  is the ratio of the density to initial density. The elastic modulus, density, and Poisson ratio of WHA are 389 GPa, 17,200  $\text{kg/m}^3$ , and 0.28, respectively, and 200 GPa, 7,840  $\text{kg/m}^3$ , and 0.3, respectively, for RHA.

## Results and Discussion

The simulated process of penetration at varying time is shown in Fig. 2 for the case when the obliquity ( $\theta$ ) is zero. At the time of 120  $\mu\text{sec}$  when the penetration event is completed, the residual length of the penetrator is comparable to the diameter of the penetrator, which phenomenon is consistent with the experimentally observed residual lengths at various obliquities and yaws [26].

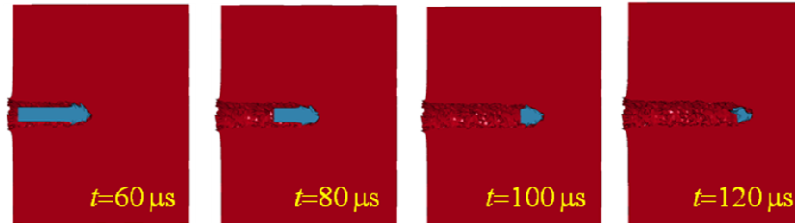


Figure 2 Process of penetration at varying time when  $\theta = 0^\circ$ .

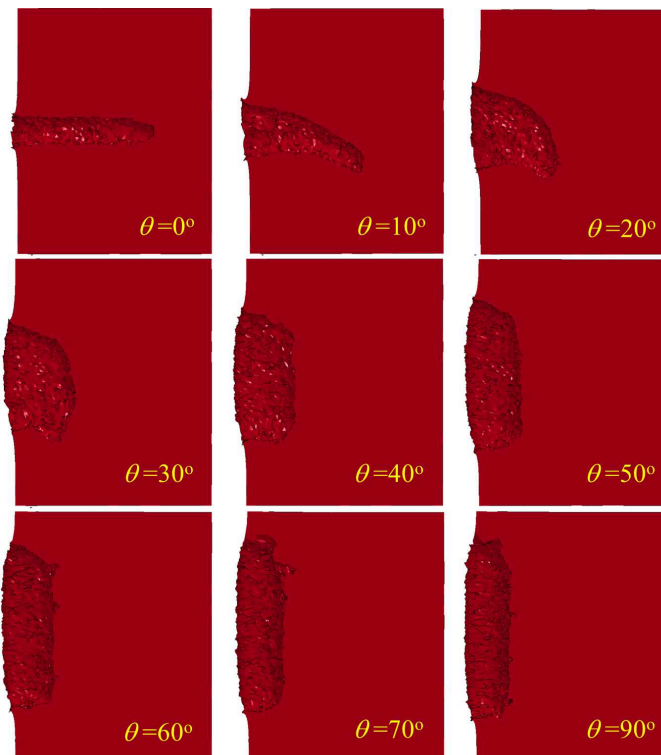


Figure 3 Shapes of the penetration holes for varying obliquity of the penetrator.

Fig. 3 shows the shapes of the final penetration holes created by the penetrator with varying obliquity. The shape of the penetration hole for the case of the obliquity of  $30^\circ$  is available in the literature (CTH calculation [4]), which is very similar to the present result.

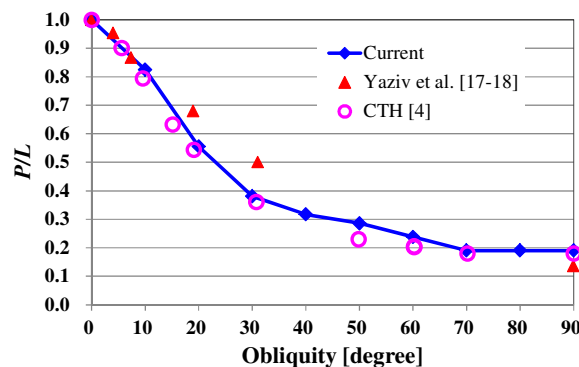


Figure 4 Depth of penetration in the RHA witness block by the WHA long-rod penetrator ( $L/D=10$ ;  $V=1.4$  km/sec) with varying obliquity.

The normalized DOP with reference to the initial length of the penetrator ( $P/L$ ) has been determined by the shortest distance from the rear surface of the witness block to the simulated penetration hole, and the result is shown in Fig. 4. Included in Fig. 4 are the experimental data adapted from References 17 and 18 (Yaziv et al. [17-18]), and the calculation result by the CTH [4]. The calculation results herein show a general agreement with the limited number of experimental data (some discrepancy at the obliquity of 20~30°). The result of the NET3D calculation is very close to that of the CTH. The features of the residual length of the penetrator when the penetration event is completed (Fig.3), the shape of the penetration hole at the obliquity of 30 (Fig. 4), and the DOP at varying obliquities (Fig. 4) indicate the effectuality of NET 3D calculation combined with the models and parameters used in the numerical analysis: the constitutive model and parameters, polynomial EOS and parameters, and the element erosion criteria.

By combining the systematic parameter study herein with the existing experiment [17-18] and calculation [4], it turns out that the DOP decreases rapidly with obliquity up to approximately 30°, decreases relatively slowly up to 70°, and shows a saturation behavior thereafter up to 90°. This result may be correlated to the change in the length component of the penetrator in the flight direction with obliquity.

### Summary

The depth of penetration (DOP) into witness block (rolled homogeneous armor) by a long-rod penetrator (tungsten heavy alloy) with varying obliquity has been investigated by NET3D code based on a 3D finite element model with the SK constitutive model and polynomial equation of state. The calculation results herein are in general agreement with the limited number of experimental data available in the literature, and are very close to the calculation result of the CTH code. The residual length of the penetrator and the shape of the penetration holes were also consistent with existing studies, indicating the effectuality of NET 3D calculation combined with the models and parameters used in the numerical analysis. By combining the systematic parameter study herein with existing experiment and calculation, it is shown that the DOP decreases rapidly with obliquity up to 30°, decreases relatively slowly up to 70°, and shows a saturation behavior thereafter up to 90°. This result may be correlated to the change in the length component of the oblique penetrator in flight direction.

### Acknowledgements

The present investigation was financially supported by the Research Program funded by the Seoul National University of Science and Technology (Grant No. 2014-023631).

### References

- [1] M. Lee, E.Y. Kim and Y.-H. Yoo: Int. J. Impact Eng. Vol. 35 (2008), p. 1636
- [2] Y.-H. Yoo and H. Shin: Int. J. Impact Eng. Vol. 30 (2004), p. 55
- [3] J.M. McGlaun and S.L. Thompson: Int. J. Impact Eng. Vol. 10 (1990), p. 351
- [4] D.J. Gee and D.L. Littlefield: Int. J. Impact Eng. Vol. 26 (2001), p. 211
- [5] J. Roopchand: Int.J. Eng..Innovative Technol. Vol. 3 (2013), p. 228.
- [6] K. Sterzelmeier, V. Brommer, L. Sinniger: IEEE Trans Magnetics Vol. 37 (2001), p. 238
- [7] H. Shin and W. Lee: Combust. Explos. Shock Waves Vol. 39 (2003), p. 470
- [8] H. Shin and W. Lee: Combust. Explos. Shock Waves Vol. 39 (2003), p. 479
- [9] H. Shin and W. Lee: Int J Impact Eng Vol. 8 (2003), p. 465
- [10] E. Liden, B. Johansson and B Lundberg: Int. J. Impact Eng. Vol. 32 (2006), p. 1696

- [11] E. Liden, O. Anderson and B Lundberg: *Int. J. Impact Eng.* Vol. 38 (2011), p. 989
- [12] E. Liden, S. Mousavi and B Lundberg: *Int. J. Impact Eng.* Vol. 40-41 (2012), p. 35
- [13] H. Shin and Y.-H. Yoo: *Combust. Explos. Shock Waves* Vol. 39 (2003), p. 591
- [14] Y.-H. Yoo, S.-H. Paik, J.-B. Kim and H. Shin: *Trans. Canadian Soc. Mech. Eng.* Vol. 37 (2013), p. 1115
- [15] Y.-H. Yoo, S.-H. Paik, J.-B. Kim and H. Shin: *Eng. Comput.* Vol. 29 (2013), p. 409
- [16] W. Lee, H.-J. Lee, and H. Shin: *J. Phys. D: Appl. Phys.* Vol. 35 (2002), p. 2676
- [17] D. Yaziv, Z. Rosenberg and J.P. Riegel III: Penetration capability of yawed long rod penetrators (Proc. 12<sup>th</sup> Int. Symp. Ballistics, San Antonio, TX, USA, p. 202, 1990)
- [18] D. Yaziv, J.D. Walker and J.P. Riegel III: Analytical model of yawed penetration in the 0 to 90 degrees range (Proc. 13<sup>th</sup> Int. Symp. Ballistics, Stockholm, Sweden, p. 17, 1992)
- [19] H. Shin, H.-J. Lee, Y.-H Yoo and W. Lee: *JSME Int. J.* Vol. 47 (2004), p. 35
- [20] H. Shin and J.B. Kim: *J. Eng. Mater. Technol.* Vol. 132 (2010), p. 021009
- [21] H. Shin and J.B. Kim: Description capability of a simple phenomenological model for flow stress of copper in an extended strain rate regime (Proc. 4th Int. Conf. on Design and Analysis of Protective Structures, Jeju, Korea, Paper No. T8-10, 2012)
- [22] G.R. Johnson and W.H. Cook: A Constitutive Model and Data for Metals Subjected to Large Strains, High Strain Rates, and High Temperatures (Proc. 7th Int. Symp. Ballistics, Den Haag, Netherlands, p. 541, 1983)
- [23] W.-S. Lee, G.-L. Xie and C.-F. Lin: *Mater. Sci. Eng.* Vol. 257 (1998), p. 256
- [24] G.T. Gray III, S.R. Chen, W. Wright and M.F. Lopez: *Constitutive Equations for Annealed Metals Under Compression at High Strain Rates and High Temperatures* (Report No. LA-12669-MS, Los Alamos National Laboratory, USA 1994)
- [25] T. Weerasooriya and P. Moy: Effect of Strain-Rate on the Deformation Behavior of Rolled-Homogeneous-Armor (RHA) Steel at Different Hardnesses, Proc. 2004 X International Congress & Exposition on Experimental & Applied Mechanics (<https://www.sem.org/Proceedings/ConferencePapers-Paper.cfm?ConfPapersPaperID=24744>).
- [26] C.E. Anderson, Jr., T. Behner, and V. Hohler: *J. Appl. Mech.* Vol. 80 (2013), p. 013801.